Biointerface Research in Applied Chemistry
Open-Access Journal (ISSN: 2069-5837)

Article
Volume 13, Issue 4, 2023, 337
https://doi.org/10.33263/BRIAC134.337

Carbon Dioxide Adsorption by a Zinc-Doped Nanocage: DFT-Based Computational Assessment of Gas Pollution Detection and Removal

Kun Harismah [1,*], Hasan Zandi [2], Moaed E. Al-Gazally [3,*]

[1] Department of Chemical Engineering, Faculty of Engineering, Universitas Muhammadiyah Surakarta, Surakarta, Indonesia; kun.harismah@ums.ac.id (K.H.);
[2] Department of Chemistry, Faculty of Science, University of Qom, Qom, Iran; h.zandi@qom.ac.ir (H.Z.);
[3] College of Medicine, University of Al-Ameed, Karbala, Iraq; moaedalgazally@yahoo.com (M.E.A.);
* Correspondence: kun.harismah@ums.ac.id (K.H.); moaedalgazally@yahoo.com (M.E.A.);
Scopus Author ID 56982926300 (K.H.); 57112488200 (M.E.A.)
Received: 4.05.2022; Accepted: 7.06.2022; Published: 11.09.2022

Abstract: The high level of carbon dioxide (CO_2) greenhouse gas exhaustion to nature could make it a serious pollutant with negative impacts on human and environmental health safety. In this regard, the current work was performed to run computational assessments on employing zinc (Zn)-doped nanocage ($C_{19}Zn$) for adsorbing the CO_2 gaseous substance to approach the detection and removal goals. Accordingly, geometries of the model systems were optimized using density functional theory (DFT) calculations to obtain the minimized energy structures besides evaluating their energy features. The obtained features approved the formation of interacting bimolecular CO_2@C19Zn complex of quantum theory of atoms in molecules (QTAIM) analysis, and the evaluated strength indicated the existence of a physical O…Zn interaction for the formation of such a complex system. Moreover, the evaluated electronic molecular orbital features indicated the possibility of detection function for the investigated system. The obtained results of this work revealed that the formation of the CO_2@$C_{19}Zn$ complex model could be supposed to conduct two functions of detection and removal of CO_2 by the investigated $C_{19}Zn$ nanocage for approaching the issues of dealing with greenhouse pollutants.

Keywords: carbon dioxide; greenhouse gas; nanocage; adsorption; DFT.

1. Introduction

Carbon dioxide (CO_2) gas has always been exhausted from both natural and industrial processes [1]. Human breathing, plant photosensitization, and industrial productions are all common resources of exhausting CO_2 gas [2-4]. Although a normal level of CO_2 is needed for the plants' photosensitization or other natural processes; however, higher levels of this gas could cause serious problems for human health and environmental safety systems [5]. Falling acidic rains, the occurrence of corrosion, and the appearance of global warming effects are only some of the negative points of the existence of high levels of CO_2 [6]. In the category of greenhouse gases, CO_2 has also been playing an important role, and its detection and removal are serious tasks to prevent gas poisoning effects [7-10]. Indeed, such issues have always affected the human health system, and they should be solved at appropriate levels [11-14]. Several efforts have been dedicated to innovating novel techniques for detecting and removing gaseous substances using different adsorbents [15-19]. In this regard, employing the

nanostructures has shown the benefits of these types of novel materials for adsorbing other atomic and molecular substances [20-22]. Indeed, the innovation of nanotechnology has provided new concepts of investigations in the materials-related science and engineering fields [23-26].

Not only the pioneering tubular nanostructure but other types of nanostructures, including layered, conical, spherical cages, and some more types, have been developed in the category of nanostructures [27-32]. Accordingly, their characterizations have shown specific electronic features for each geometrically recognized nanostructures employed for various applications [33-35]. Moreover, earlier works indicated the impacts of atomic dopants for preparing nanostructures with more specified electronic features [36-38]. Such atomic doped regions of nanostructures could provide an active site for conducting more efficient interactions with other substances [39-41]. Metal atoms have the advantage of dopants by supplying more vacant electronic orbitals for adsorbing other substances through their lone pair of electron heads [42-44]. Accordingly, the hypothesis of CO_2 adsorbing by zinc (Zn)-doped nanocage has been investigated in the current work for approaching the goals of detection and removal of this gaseous substance with the assistance of nanostructures. Indeed, the topic of gas adsorption is important because of various aspects of such processes to innovate novel materials for working in gas sensor fuctions or to learn details of such interacting systems [45-47]. In this case, the topic has become a non-stop topic for investigating new features of such expected functions [48-50]. Several works indicated such importance because every time exhausting pollutants to nature threaten human and environmental health, it is a must to provide more helpful insights about these unsolved health systems issues [51-54]. It is obvious that further investigations are required to learn details of nano-based systems and human health issues [55-60].

In the current research work, density functional theory (DFT) calculations were performed to optimize the model systems, besides evaluating their required information for examining the specified hypothesis. All results were used for conducting the computational assessments of CO_2 adsorption by the Zn-doped nanocage. To this aim, a representative model of nanocage (Figure 1) was investigated for adsorbing the CO_2 molecular substance, in which the original carbon-composed nanocage was doped by one Zn atom to provide a Zn-doped active site for participating in interactions with the external CO_2 molecule. The singular and bimolecular models were analyzed to see the benefits of employing such a model system for detecting and removing CO_2 gaseous substances for dealing with the greenhouse gas pollutants in the environment. The investigated models and the evaluated features of this work are exhibited in Figures 1 and 2 and Table 1.

2. Materials and Methods

The singular models of CO_2 and $C_{19}Zn$ nanocage were optimized to prepare the required parental materials for the investigation of this work. For building the molecular model cage, one carbon atom of the carbon-20 model was substituted by one Zn atom to bring the $C_{19}Zn$ model. Next, the bimolecular formation of the $CO_2@C_{19}Zn$ complex was investigated by performing re-optimization calculations on already optimized singular models. By examining all possible configurations of interacting molecular systems, a final model of such $CO_2@C_{19}Zn$ complex was obtained (Figure 1). In this regard, the evaluated features of electrostatic potential (ESP) surfaces approved the existence of such molecular interactions, in which the Zn-doped region of singular nanocage was in blue color resembling a positive atomic site for interacting

with the O head of CO_2 in yellow color resembling the negative atomic site. Accordingly, the evaluated ESP of the bimolecular model approved the existence of such an interacting complex by representing a continuous ESP surface distribution. To analyze the interacting system, the features of the quantum theory of atoms in molecules (QTAIM) were evaluated to show the existence and strength of involving interaction (Table 1) [61].

Moreover, values of the adsorption energy (E_{Ads}) and energy levels of the highest occupied and the lowest unoccupied molecular orbitals (HOMO and LUMO) were evaluated for the models. The values of energy gap (E_{Gap}) and Fermi energy (E_{Fermi}) were also evaluated accordingly. To show variations of electronic molecular orbitals features, diagrams of the density of states (DOS) were illustrated for the models (Figure 2). All computations of this work were performed at the wB97XD/6-31+G(d,p) level of DFT calculations using the Gaussian program [62]. To approach the goal of this work to do computational assessment of CO_2 adsorption by a Zn-doped nanocage, the results were provided by DFT calculations as benefits of employing the computational tools for solving problems in science and engineering [63-67].

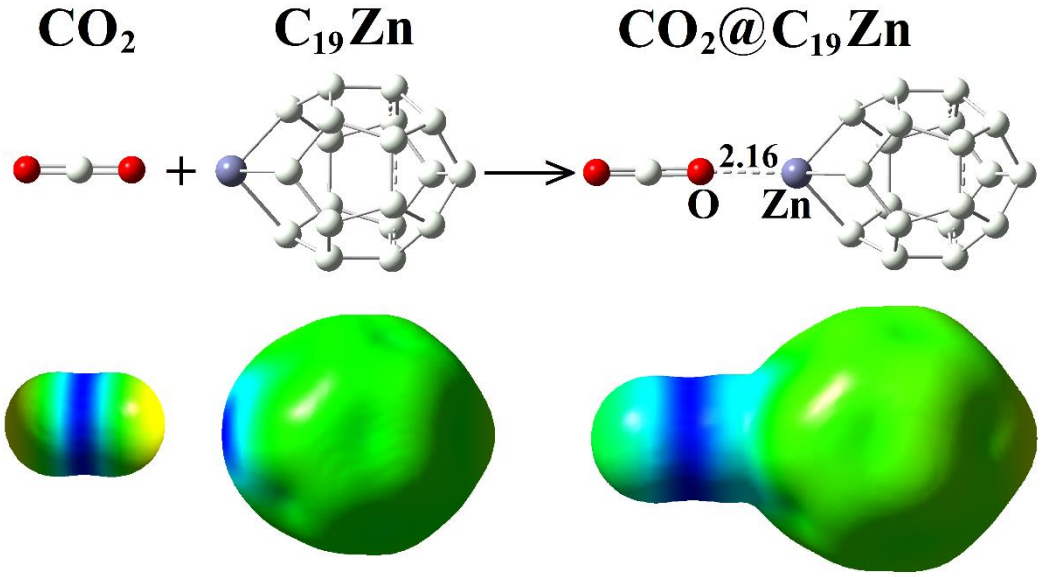

Figure 1. Representation of the models of this work and their ESP surfaces.

Table 1. The evaluated features of the models.[1]

Model	Int.	Dis.	Rho	Del^2-Rho	H	E_{Ads}	HOMO	LUMO	E_{Gap}	E_{Fermi}
CO_2@C_{19}Zn	O…Zn	2.16	0.044	0.23	-0.036	-9.62	-7.88	-1.32	6.56	-4.60
CO_2	n/a	n/a	n/a	n/a	n/a	n/a	-12.69	1.35	14.04	-5.67
C_{19}Zn	n/a	n/a	n/a	n/a	n/a	n/a	-8.18	-1.73	6.45	-4.96

[1]The units: Dis. (Å); Rho, Del^2-Rho, and H (au); E_{Ads} (kcal/mol); HOMO, LUMO, E_{Gap}, and E_{Fermi} (eV).

3. Results and Discussion

In this work, computational assessments at the level of DFT calculations were performed to analyze the process of CO_2 adsorption by a Zn-doped nanocage (Figure 1). To approach this goal, geometries of the singular models were optimized to prepare the parental models of this work. Next, geometries of combined CO_2 and C_{19}Zn molecules were re-optimized to reach the bimolecular model of the CO_2@C_{19}Zn complex. Indeed, all possible geometries were examined to reach a final possible configuration for forming the CO_2@C_{19}Zn complex. The complex model was analyzed by evaluating various features for this purpose. As indicated by the evaluated results of Table 1, the interacting complex model occurred by

involving one O…Zn interaction (Int.) with the distance (Dis.) of 2.16 Å. The QTAIM features, including the density of all electrons (Rho), Laplacian of electron density (Del^2-Rho), and energy density (H), were evaluated to recognize the nature of O…Zn interaction [47-49]. To this point, the obtained values of 0.044, 0.23, and -0.036 for Rho, Del^2-Rho, and H, indicated reasonable strength of the interaction as categorized in the physical interactions. Based on this achievement, the formation of the CO_2@C_{19}Zn complex could be achievable, and the involved physical interaction could make it usable for reversible adsorption processes. Accordingly, the evaluated strength of the complex was notable by calculating the value of -9.62 kcal/mol for E_{Ads} for the adsorption process of CO_2 at the surface of the C_{19}Zn nanocage. As a consequence, the obtained details of interacting features approved the hypothesis of CO_2 adsorption by the C_{19}Zn cage to yield the formation of the bimolecular CO_2@C_{19}Zn complex. Formations of interacting complexes could help learn about the materials' features for involvement in the adsorption processes. Recognizing the atomic features and those atoms with contributions to interactions could help develop new materials for the specified purposes. As mentioned earlier about the role of the atomic doped region for activating the surface for participating in interactions, such a role was seen for the investigated nanocage by the role of the Zn-doped region for conducting the interaction process. To describe this observation more, the availability of plenty of vacant atomic orbitals of the Zn atom could help this atom to adsorb the lone pairs of electrons of the O head of CO_2.

In comparison with the original carbon atom surface, the existence of such an atom could help the surface to be a host for adsorbing the external substance. Accordingly, a direct O...Zn interaction was observed for the interacting CO_2@C_{19}Zn complex to yield a relaxed configuration of CO_2 at the surface of the nanocage. Based on the ESP features, the rest of the nanocage were in the green color resembling a neutral surface, whereas the blue color showed the doped region resembling a charged point at the surface of the nanocage. Additionally, the middle part of the O=C=O molecule was also in the blue color, but the O head was in the yellow to semi-red color, showing the possibility of the formation of interactions between the O head of CO_2 and the Zn-doped region of nanocage. The next results approved such expectations, especially by the obtained features of QTAIM analysis. By learning about the role of investigated nanocages for adsorbing CO_2 to approach the removal function, it should be known how to recognize the formation of such a complex model for conducting the detection function. To approach this goal, monitoring the electronic molecular orbital features of the models prior to/after complex formation could help to conduct such detection function, as shown by the illustrated DOS diagrams in Figure 2.

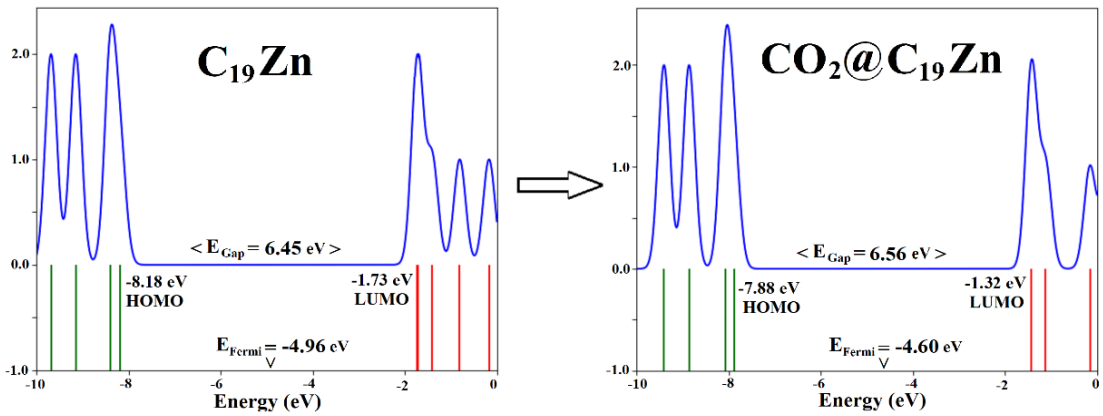

Figure 2. The illustrated DOS diagrams of the models.

In this regard, the values of HOMO and LUMO, resembling energy levels of the electron transferring process, were evaluated. HOMO could imply the level of electron-donating, and LUMO could imply the level of electron-accepting. Accordingly, details of the electron transferring processes inside a molecular system or between two molecular systems could be found. It is worth mentioning that the targeted HOMO and LUMO levels are those frontier molecular orbitals, in which several other occupied and unoccupied molecular orbitals are before HOMO and after LUMO, respectively. As shown in Figure 2, the illustrated DOS diagrams exhibited variations of such electronic molecular orbitals. The value of HOMO was found to be -12.69 and -8.18 eV for each of the singular models of CO_2 and $C_{19}Zn$ nanocage, and the value of LUMO was found to be 1.35 and -.173 eV for the mentioned models. In this case, different values of each level could help the models participate in electron transfer processes. Inside the molecular systems, energy distances of HOMO and LUMO levels were identified by the value of $E_{Gap,}$ showing 14.04 and 6.45 eV for each of the singular CO_2 and $C_{19}Zn$ models. The value of EFermi identified average values of HOMO and LUMO; -5.67 and -4.96 eV for the singular CO_2 and $C_{19}Zn$ models. These results indicated that the models could be detectable by each other by their different values of electronic molecular orbitals features.

Accordingly, the obtained parallel results for the interacting $CO_2@C_{19}Zn$ complex model affirmed such achievement for approaching the detection function. Levels of HOMO and LUMO were changed in the complex model compared to the singular models, and measuring their features could be helpful for detecting the formation of the bimolecular complex. The illustrated diagrams of DOS for the singular $C_{19}Zn$ model and the bimolecular $CO_2@C_{19}Zn$ complex affirmed such achievement of the possibility of approaching the detection function of investigated $C_{19}Zn$ nanocage for the external CO_2 gas. As mentioned by the values of HOMO and LUMO for each of the singular models, the evaluated E_{Gap} of CO_2 was wider than that of the $C_{19}Zn$ nanocage. The observed E_{Gap} of the complex was wider than that of singular nanocage and narrower than that of singular CO_2, revealing the impacts of the occurrence of interactions on the electronic molecular orbital levels.

Moreover, the level of E_{Fermi} was also changed in the complex model, affirming the mentioned impacts of interactions. In this regard, approaching the detection function could be achievable for the investigated systems to show the adsorption of CO_2 at the surface of the $C_{19}Zn$ nanocage. Consequently, the current computational assessments indicated that the investigated $C_{19}Zn$ cage was suitable for working in two functions detection and removal of CO_2 gas by forming an interacting $CO_2@C_{19}Zn$ complex. Comparing the current results with another parallel work showed the benefit of employing this model for adsorbing the CO_2 substance [45]. Accordingly, the model could be proposed for further investigations regarding the importance of dealing with the CO_2 greenhouse gas to maintain human and environmental health safety.

4. Conclusions

This work's computational assessments were performed based on DFT calculations to recognize the features of CO_2 adsorption by a Zn-doped nanocage. To this aim, geometries of the singular CO_2 and $C_{19}Zn$ models and their interacting bimolecular $CO_2@C_{19}Zn$ complex were optimized to obtain minimized energy systems. Next, their interacting features and energy details were obtained. One O…Zn interaction was found for the formation of the complex model, and the QTAIM analysis indicated it as a physical interaction. Such obtained interaction

features helped the model form a reversible system, making the reuse of nanocage possible. Moreover, the features of electronic molecular orbitals indicated variations of such energy levels after complex formation. Accordingly, evaluating such features helped to make detection of adsorbed CO_2 ad the surface of the nanocage. It was shown that the Zn-doped atom had a significant role in conducting participation of nanocage in imitation with the CO_2 substance resulting in the interacting CO_2@C_{19}Zn nanocage. In this regard, two functions of detection and removal of CO_2 with the assistance of C_{19}Zn nanocage were found to make suitable the investigated model for further investigations on dealing with the greenhouse gases pollutants.

Funding

This research received no external funding.

Acknowledgments

This research has no acknowledgment.

Conflicts of Interest

The authors declare no conflict of interest.

References

1. Dosch, M.P. Treating increased inspired carbon dioxide. *Anesthesia & Analgesia* **2021**, *133*, e23–e24, https://doi.org/10.1213/ane.0000000000005614.
2. Watson, M.; Ionescu, M.F.; Sylvester, K.; Fuld, J. Minute ventilation/carbon dioxide production in patients with dysfunctional breathing. *European Respiratory Review* **2021**, *30*, 200182, https://doi.org/10.1183/16000617.0182–2020.
3. Lowther, S.D.; Dimitroulopoulou, S.; Foxall, K.; Shrubsole, C.; Cheek, E.; Gadeberg, B.; Sepai, O. Low level carbon dioxide indoors–a pollution indicator or a pollutant? a health–based perspective. *Environments* **2021**, *8*, 125, https://doi.org/10.3390/environments8110125.
4. Tutmez, B. Interpreting relationships between pollutants and carbon dioxide emitted into air from industries in Serbia. *Journal of Engineering Management and Competitiveness* **2021**, *11*, 115–123, https://doi.org/10.5937/jemc2102115t.
5. Wang, G.; Mulmi, S.; Chen, H.; Thangadurai, V. Perovskite–type semiconductors for detecting ppm level of carbon dioxide. *Ionics* **2022**, *28*, 463–476, https://doi.org/10.1007/s11581–021–04336–y.
6. Terlouw, T.; Bauer, C.; Rosa, L.; Mazzotti, M. Life cycle assessment of carbon dioxide removal technologies: a critical review. *Energy & Environmental Science* **2021**, *14*, 1701–1721, https://doi.org/10.1039/d0ee03757e.
7. Vaeli, N. Laboratory study of effective factors on how to extract carvacrol from oliveria decumbens plant with the help of supercritical fluid CO_2 and using ultrasound waves. *Eurasian Journal of Science and Technology* **2022**, *2*, 32–43, https://doi.org/10.22034/ejst.2022.1.3.
8. Petrovic, B.; Gorbounov, M.; Soltani, S.M. Influence of surface modification on selective CO_2 adsorption: a technical review on mechanisms and methods. *Microporous and Mesoporous Materials* **2021**, *312*, 110751, https://doi.org/10.1016/j.micromeso.2020.110751.
9. Keshavarz, L.; Ghaani, M.R.; MacElroy, J.D.; English, N.J. A comprehensive review on the application of aerogels in CO2–adsorption: materials and characterisation. *Chemical Engineering Journal* **2021**, *412*, 128604, https://doi.org/10.1016/j.cej.2021.128604.
10. Ariaei, S.; Basiri, H.; Ramezani, M. Selective adsorption function of B16C16 nano–cage for H_2O, CO, CH_4 and NO_2. *Advanced Journal of Chemistry–Section B: Natural Products and Medical Chemistry* **2020**, *2*, 18–25, https://doi.org/10.33945/sami/ajcb.2020.1.4.
11. Kumar, A.; Gupte, B.; Shangloo, P. Effect of nicotine smoke on genitourinary organs of male albino rats: an experimental study. *International Journal of Scientific Research in Dental and Medical Sciences* **2021**, *3*, 141–146, http://doi.org/10.30485/ijsrdms.2021.296503.1177.

12. Kumar, S.; Sah, S.P.; Kumar, D.; Arora, M.; Iqbal, S.; Sharma, S. Association of oxidative stress with renal function in cigarette smokers. *International Journal of Scientific Research in Dental and Medical Sciences* **2022,** *4*, 33–37, http://doi.org/10.30485/ijsrdms.2022.325504.1243.
13. Nezhadnasrollah, F.; Fotovat, F.; Yousefi, H.; Fatahi, M.; Rasoolinia, M. The effect of four disc-shaped polishing systems on the surface roughness and micro-hardness of clearfil AP-X esthetics composite resin. *International Journal of Scientific Research in Dental and Medical Sciences* **2022,** *4*, 16–20, http://doi.org/10.30485/ijsrdms.2022.331297.1257.
14. Singh, A.; Brar, R.; Virk, A.; Verma, S.K. The impact of metabolic syndrome on clinical outcome of COVID-19 patients: a retrospective study. *International Journal of Scientific Research in Dental and Medical Sciences* **2021,** *3*, 161–165, http://doi.org/10.30485/ijsrdms.2021.307324.1201.
15. Ariaei, S. DFT approach on arsine and phosphine gases adsorption at the surface of B16C16 nanocluster. *Lab–in–Silico* **2020**, *1*, 44–49.
16. Zarifi, K.; Rezaei, F.; Seyed Alizadeh, S.M. A model of FeN–decorated BeO layer particle for CO gas adsorption. *Main Group Chemistry* **2022**, *21*, 125–132, https://doi.org/10.3233/mgc-210100.
17. Godarzi, M.; Ahmadi, R.; Ghiasi, R. Adsorption of 3–picrylamino–1,2,4–triazole on C60 surface as a green fuel: DFT studies. *Asian Journal of Green Chemistry* **2020**, *4*, 220–230, https://doi.org/10.22034/ajgc/2020.2.9.
18. Jalali Sarvestani, M.; Ahmadi, R. A comprehensive DFT study on the adsorption of tetryl on the surface of graphene. *Asian Journal of Green Chemistry* **2020**, *4*, 269–282, https://doi.org/10.22034/ajgc/2020.3.4.
19. Shehni, S.; Tabatabaee Ghomscheh, S. Assessment of MoTiO3/GO integrated photocatalyst for converting CO2 to methanol. *Chemical Methodologies* **2022**, *6*, 699–709, https://doi.org/10.22034/chemm.2022.339764.1502.
20. Rezaei–Aghdam, E.; Shamel, A.; Khodadadi–Moghaddam, M.; Ebrahimzadeh Rajaei, G.; Mohajeri, S. Hydrothermal synthesis of ZnO nanoparticles and comparison of its adsorption characteristics with the natural adsorbent (mango peel). *Asian Journal of Nanosciences and Materials* **2021**, *4*, 188–200, https://doi.org/10.26655/ajnanomat.2021.3.2.
21. Harismah, K.; Nayini, M.M.; Montazeri, S.; Ariaei, S.; Nouraliei, M. DFT investigation of SiO2 nanotube for adsorption of methyl–and propyl–paraben. *Main Group Chemistry* **2021**, *20*, 355–363, https://doi.org/10.3233/mgc-210052.
22. Ariaei, S.; Fallahpour, F.; Basiri, H.; Moradi, R. A DFT study of H2 molecule adsorption at the fullerene–like boron carbide nanocage. *Advanced Journal of Science and Engineering* **2021**, *2*, 18–22.
23. Ahmed, H.; Abdulrahman, N. Effect of magnetic field on the preparation of Cu doped zinc oxide nanostructures in different temperatures. *Eurasian Chemical Communications* **2021**, *3*, 443–451, https://doi.org/10.22034/ecc.2021.282390.1171.
24. Mirzaei, M.; Rasouli, A.H.; Saedi, A. HOMO–LUMO photosensitization analyses of coronene–cytosine complexes. *Main Group Chemistry* **2021**, *20*, 565–573, https://doi.org/10.3233/mgc-210078.
25. Bodaghi, A.; Mirzaei, M.; Seif, A.; Giahi, M. A computational NMR study on zigzag aluminum nitride nanotubes. *Physica E: Low–dimensional Systems and Nanostructures* **2008**, *41*, 209–212, https://doi.org/10.1016/j.physe.2008.06.023.
26. Mammadova, S.; Nasibova, A.; Khalilov, R.; Mehraliyeva, S.; Valiyeva, M.; Gojayev, A.; Zhdanov, R.; Eftekhari, A. Nanomaterials application in air pollution remediation. *Eurasian Chemical Communications* **2022**, *4*, 160–166, https://doi.org/10.22034/ecc.2022.315481.1265.
27. Zou, Y.; Xu, J.; Chen, K.; Chen, J. Advances in nanostructures for high-performance triboelectric nanogenerators. *Advanced Materials Technologies* **2021**, *6*, 2000916, https://doi.org/10.1002/admt.202000916.
28. Ghotekar, S.; Dabhane, H.; Pansambal, S.; Oza, R.; Tambade, P.; Medhane, V. A review on biomimetic synthesis of Ag2O nanoparticles using plant extract, characterization and its recent applications. *Advanced Journal of Chemistry–Section B: Natural Products and Medical Chemistry* **2020**, *2*, 102–111, https://doi.org/10.22034/ajcb.2020.107810.
29. Jasem, N.; Al–Quzweny, M.; Alsammarraie, A. Spectroscopic investigation of carbon nanostructures. *Chemical Methodologies* **2022**, *6*, 237–245, https://doi.org/10.22034/chemm.2022.322390.1416.
30. Vardini, M.; Abbasi, N.; Kaviani, A.; Ahmadi, M.; Karimi, E. Graphite electrode potentiometric sensor modified by surface imprinted silica gel to measure valproic acid. *Chemical Methodologies* **2022**, *6*, 398–408, https://doi.org/10.22034/chemm.2022.328620.1437.

31. Ghotekar, S.; Pagar, T.; Pansambal, S.; Oza, R. A review on green synthesis of sulfur nanoparticles via plant extract, characterization and its applications. *Advanced Journal of Chemistry–Section B: Natural Products and Medical Chemistry* **2020**, *2*, 128–143, https://doi.org/10.22034/ajcb.2020.109501.
32. Shahzad, H.; Ahmadi, R.; Sheshmani, S. Investigating the performance of nano structure C60 as nano–carriers of anticancer cytarabine, a DFT study. *Asian Journal of Green Chemistry* **2020**, *4*, 355–366, https://doi.org/10.22034/ajgc.2020.97394.
33. Baghernejad, B.; Nazari, L. Synthesis of indeno [1,2–b] pyridine derivatives in the precense of Nano CeO2/ZnO. *Eurasian Chemical Communications* **2021**, *3*, 319–326, https://doi.org/10.22034/ecc.2021.277002.1145.
34. Farajzadeh, S.; Najafi Moghadam, P.; Khalafy, J. Removal of colored pollutants from aqueous solutions with a poly Schiff–base based on melamine–modified MWCNT. *Asian Journal of Green Chemistry* **2020**, *4*, 397–415, https://doi.org/10.22034/ajgc.2020.100567.
35. Janighorban, M.; Rasouli, N.; Sohrabi, N.; Ghaedi, M. Use of central composite design and surface modeling for cadmium (ii) ions removal from aqueous environment using novel modified layer double hydroxide. Asian *Journal of Green Chemistry* **2021**, *5*, 151–175, https://doi.org/10.22034/ajgc.2021.118922.
36. Anafcheh, M. A comparison between density functional theory calculations and the additive schemes of polarizabilities of the Li–F–decorated BN cages. *Journal of Applied Organometallic Chemistry* **2021**, *1*, 125–133, https://doi.org/10.22034/jaoc.2021.292384.1027.
37. Adole, V. Computational chemistry approach for the investigation of structural, electronic, chemical and quantum chemical facets of twelve biginelli adducts. *Journal of Applied Organometallic Chemistry* **2021**, *1*, 29–40, https://doi.org/10.22034/jaoc.2021.278598.1009.
38. Amouzad Mahdiraji, E. Evaluation of corona charge positive and negative impulses on polymeric surfaces and simulation of impact rate. *Eurasian Journal of Science and Technology* **2021**, *1*, 234–241, https://doi.org/10.22034/jstr.2021.289237.1038.
39. Bayat, P.; Yousefi, M. Density functional theory investigation of lead adsorption by a graphene layer. *Advanced Journal of Science and Engineering* **2022**, *3*, 18–22.
40. Iranimanesh, A.; Yousefi, M.; Mirzaei, M. DFT approach on SiC nanotube for NO_2 gas pollutant removal. *Lab–in–Silico* **2021**, *2*, 38–43.
41. Kouchaki, A.; Gülseren, O.; Hadipour, N.; Mirzaei, M. Relaxations of fluorouracil tautomers by decorations of fullerene–like SiCs: DFT studies. *Physics Letters A* **2016**, *380*, 2160–2166, https://doi.org/10.1016/j.physleta.2016.04.037.
42. Al–Haideri, L.M.; Cakmak, N. Electronic and structural features of uranium–doped graphene: DFT study. *Main Group Chemistry* **2022**, *21*, 295–301, https://doi.org/10.3233/mgc-210143.
43. Islam, M.; Paul, S.; Kumer, A.; Sarker, M. Computational approach of palladium (II) complex ions with binuclear diamine ligands thermo–physical, chemical, and biological properties: a dft study. *Asian Journal of Nanosciences and Materials* **2020**, *3*, 67–81, https://doi.org/10.26655/ajnanomat.2020.1.7.
44. Rida, Z.; Hassan, S.; Awad, S. Synthesis and characterization of new inorganic complexes and evaluation their corrosion inhibiter. *Chemical Methodologies* **2022**, *6*, 347–356, https://doi.org/10.22034/chemm.2022.326331.1431.
45. Zou, Y.H.; Huang, Y.B.; Si, D.H.; Yin, Q.; Wu, Q.J.; Weng, Z.; Cao, R. Porous metal–organic framework liquids for enhanced CO_2 adsorption and catalytic conversion. *Angewandte Chemie* **2021**, *133*, 21083–21088, https://doi.org/10.1002/ange.202107156.
46. Jalali Sarvestani, M.; Ahmadi, R. Adsorption of TNT on the surface of pristine and N–doped carbon nanocone: a theoretical study. *Asian Journal of Nanosciences and Materials* **2020**, *3*, 103–114, https://doi.org/10.26655/ajnanomat.2020.2.2.
47. Ariaei, S. DFT calculations of a cubic B4N4 cubane–like particle for CO gas adsorption. *Advanced Journal of Science and Engineering* **2021**, *2*, 93–98.
48. Kolbadinezhad, R.; Amouzad Mahdiraji, E. Inhalation exposure to dust pollution in the workplace. *Eurasian Journal of Science and Technology* **2021**, *1*, 75–82, https://doi.org/10.22034/jstr.2021.285211.1018.
49. Zandi, H.; Harismah, K. Density functional theory analyses of non–covalent complex formation of 6–thioguanine and coronene. *Lab–in–Silico* **2021**, *2*, 57–62.
50. Brous, A. Color conversion filters. *Eurasian Journal of Science and Technology* **2021**, *1*, 83–88, https://doi.org/10.22034/jstr.2021.284999.1016.
51. Mohamed, M. Removal of methylene blue from aqueous solution using Egyptian date pits. *Asian Journal of Nanosciences and Materials* **2021**, *4*, 113–124, https://doi.org/10.26655/ajnanomat.2021.2.2.

52. Kreydie, S.; Al–Abdaly, B. Synthesis, characterization and evaluation of inhibition corrosion of bacterial cellulose/metal oxides nanocomposites. *Eurasian Chemical Communications* **2021**, *3*, 706–714, https://doi.org/10.22034/ecc.2021.299439.1216.
53. Bashandeh, Z.; Dehno Khalaji, A. An efficient removal of methyl green dye by adsorption onto new modified chitosan Schiff base. *Asian Journal of Nanosciences and Materials* **2021**, *4*, 274–281.
54. Mohammed, R.; Saleh, K. A novel conducting polyamic acid/nanocomposite coating for corrosion protection. *Eurasian Chemical Communications* **2021**, *3*, 715–725, https://doi.org/10.22034/ecc.2021.296065.1206.
55. Wikantyasning , E.R.; Kalsum, U.; Nurfiani, S.; Da'I, M.; Cholisoh, Z. Allylamine-conjugated polyacrylic acid and gold nanoparticles for colorimetric detection of bacteria. *Materials Science Forum* **2021**, *1029*, 137–144, https://doi.org/10.4028/www.scientific.net/MSF.1029.137.
56. Wikantyasning , E.R.; Mutmainnah, M.; Cholisoh, Z.; Hairunisa, I.; Bakar, M.F.A.; Da'i, M. Preparation of hydrogel nanocomposite containing gold nanoparticles with unique swelling/deswelling properties. *Rasayan Journal of Chemistry* **2019**, *12*, 1857–1863, https://doi.org/10.31788/RJC.2019.1245209.
57. Chukwuanukwu, T.; Afiadigwe, E.; Apakama, A.; Chukwuanukwu, R.; Uchechukwu Nwankwo, E.; Ilokanuno, C. Epidemiology of cleft lip and palate in nigeria: a data-based study. *International Journal of Scientific Research in Dental and Medical Sciences* **2021**, *3*, 73–77, https://doi.org/10.30485/IJSRDMS.2021.278259.1137.
58. Makani Bassakouahou, J.; Kouala Landa, C.; Kimbally-Kaky, E.; Bakekolo, P.; Ellenga Mbolla, B.; Ikama, M. Aortic remodeling and human immunodeficiency virus infection: two case reports. *International Journal of Scientific Research in Dental and Medical Sciences* **2021**, *3*, 190–192, https://doi.org/10.30485/ijsrdms.2021.306038.1194.
59. Rather, A.; Wani, G.M.; Robbani, I. Multidetector-row computed tomography and colour doppler imaging in the evaluation of patients with extrahepatic portal hypertension: a prospective study. *International Journal of Scientific Research in Dental and Medical Sciences* **2021**, *3*, 86–93, https://doi.org/10.30485/ijsrdms.2021.285539.1153.
60. Ulasi, T.; Nri-Ezedi, C.; Ofiaeli, O.; Chijioke, E. Novel cases of diamond blackfan anaemia in two nigerian toddlers: roadmap for care in resource-limited nations. *International Journal of Scientific Research in Dental and Medical Sciences* **2021**, *3*, 101–104, https://doi.org/10.30485/ijsrdms.2021.282666.1148.
61. Rad, A.S.; Aghaei, S.M.; Poralijan, V.; Peyravi, M.; Mirzaei, M. Application of pristine and Ni–decorated $B_{12}P_{12}$ nano–clusters as superior media for acetylene and ethylene adsorption: DFT calculations. *Computational and Theoretical Chemistry* **2017**, *1109*, 1–9, https://doi.org/10.1016/j.comptc.2017.03.030.
62. Frisch, M.J.; Trucks, G.W.; Schlegel, H.B. et al. Gaussian 09 program. *Gaussian Inc*. **2009,** Wallingford, CT.
63. Harismah, K.; Hajali, N.; Mirzaei, M.; Salarrezaei, E. Quantum processing of cytidine derivatives and evaluating their in silico interactions with the COVID–19 main protease. *Main Group Chemistry* **2022**, *21*, 263–270, https://doi.org/10.3233/mgc-210134.
64. Sharma, R.; Singh, M.K.K.; Ghatpande, N.; Shaikh, M.; Jadhav, J.; Murugavel, S.; Kant, R. Synthesis, crystal structure, Hirshfeld surface, crystal voids, energy frameworks, DFT and molecular docking analysis of (2,6–dimethoxyphenyl)acetic acid. *Advanced Journal of Chemistry–Section B: Natural Products and Medical Chemistry* **2022**, *4*, 1–16, https://doi.org/10.22034/ajcb.2022.320258.1102.
65. Amouzad Mahdiraji, E.; Sedghi Amiri, M. Adaptive control of network frequency by doubly–fed induction generators using a data–driven method. *Eurasian Journal of Science and Technology* **2021**, *1*, 89–103, https://doi.org/10.22034/jstr.2021.130260.
66. Venkatesh, G.; Sheena mary, Y.; Shymamary, Y.; Palanisamy, V.; Govindaraju, M. Quantum chemical and molecular docking studies of some phenothiazine derivatives. *Journal of Applied Organometallic Chemistry* **2021**, *1*, 148–158, https://doi.org/10.22034/jaoc.2021.303059.1033.
67. Yaraghi, A.; Ozkendir, O.M.; Mirzaei, M. DFT studies of 5–fluorouracil tautomers on a silicon graphene nanosheet. *Superlattices and Microstructures* **2015**, *85*, 784–788, https://doi.org/10.1016/j.spmi.2015.05.053.